



## OPEN ACCESS

## EDITED BY

Jeehee Youn,  
Hanyang University, Republic of Korea

## REVIEWED BY

Laurence Morel,  
The University of Texas Health Science  
Center at San Antonio, United States  
Susan Swain,  
University of Massachusetts Medical  
School, United States

## \*CORRESPONDENCE

Sun Jung Kim  
✉ [sjkim@northwell.edu](mailto:sjkim@northwell.edu)

RECEIVED 16 June 2023

ACCEPTED 21 August 2023

PUBLISHED 06 September 2023

## CITATION

Ramirez De Oleo I, Kim V,  
Atisha-Fregoso Y, Shih AJ,  
Lee K, Diamond B and Kim SJ (2023)  
Phenotypic and functional  
characteristics of murine CD11c+  
B cells which is suppressed  
by metformin.  
*Front. Immunol.* 14:1241531.  
doi: 10.3389/fimmu.2023.1241531

## COPYRIGHT

© 2023 Ramirez De Oleo, Kim,  
Atisha-Fregoso, Shih, Lee, Diamond and Kim.  
This is an open-access article distributed  
under the terms of the [Creative Commons  
Attribution License \(CC BY\)](https://creativecommons.org/licenses/by/4.0/). The use,  
distribution or reproduction in other  
forums is permitted, provided the original  
author(s) and the copyright owner(s) are  
credited and that the original publication in  
this journal is cited, in accordance with  
accepted academic practice. No use,  
distribution or reproduction is permitted  
which does not comply with these terms.

# Phenotypic and functional characteristics of murine CD11c+ B cells which is suppressed by metformin

Ivan Ramirez De Oleo<sup>1</sup>, Vera Kim<sup>1</sup>, Yemil Atisha-Fregoso<sup>1</sup>,  
Andrew J. Shih<sup>2</sup>, Kyungwoo Lee<sup>1,3</sup>, Betty Diamond<sup>1,4</sup>  
and Sun Jung Kim<sup>1,4\*</sup>

<sup>1</sup>Center for Autoimmune, Musculoskeletal and Hematopoietic Diseases, The Feinstein Institutes for Medical Research, Manhasset, NY, United States, <sup>2</sup>Center for Genomics and Human Genetics, The Feinstein Institutes for Medical Research, Manhasset, NY, United States, <sup>3</sup>Department of Biology at Hofstra University, Hempstead, NY, United States, <sup>4</sup>Department of Molecular Medicine, Donald and Barbara Zucker School of Medicine at Hofstra University/Northwell, Hempstead, NY, United States

Since the description of age-associated or autoimmune-associated B cells (ABCs), there has been a growing interest in the role of these cells in autoimmunity. ABCs are differently defined depending on the research group and are heterogeneous subsets. Here, we sought to characterize ABCs in Sle1/2/3 triple congenic (TC) mice, which is a well accepted mouse model of lupus. Compared to follicular (FO) B cells, ABCs have many distinct functional properties, including antigen presentation. They express key costimulatory molecules for T cell activation and a distinct profile of cytokines. Moreover, they exhibit an increased capacity for antigen uptake. ABCs were also compared with germinal center (GC) B cells, which are antigen activated B cell population. There are several phenotypic similarities between ABCs and GC B cells, but GC B cells do not produce proinflammatory cytokines or take up antigen. While T cell proliferation and activation is induced by both FO B and ABCs in an antigen-dependent manner, ABCs induce stronger T cell receptor signaling in naïve CD4+ T cells and preferentially induce differentiation of T follicular helper (Tfh) cells. We found that ABCs exhibit a distinct transcriptomic profile which is focused on metabolism, cytokine signaling and antigen uptake and processing. ABCs exhibit an increase in both glycolysis and oxidative phosphorylation compared to FO B cells. Treatment of ABCs with metformin suppresses antigen presentation by decreasing antigen uptake, resulting in decreased Tfh differentiation. Taken together, these findings define a fundamental connection between metabolism and function within ABCs.

## KEYWORDS

follicular T helper cells (Tfh), systemic lupus erythematosus (SLE), age-associated B cells (ABCs), mouse model, metabolism, autoimmune diseases

## Introduction

B cells play critical roles in host defense through their capacity to produce antibodies and cytokines as well as present antigens to T cells. Uncontrolled B cell activation or reactivity to self-antigens contributes to deleterious autoimmune responses. In addition to conventional B2 and B1 cells, a distinct and unusual B cell subset has been identified in humans and mice. It is characterized by expression of the integrin, CD11c, and T-box transcription factor (T-bet) and lack of the follicle-homing chemokine receptor (CXCR5) and CD21 (1, 2). They are termed age-associated or autoimmune-associated B cells (ABCs). Initial studies characterized ABCs by expression of CD11c (alone or with CD11b) in aged mice, and in multiple mouse models for systemic lupus erythematosus (SLE) expanded (2–4). Similarly, ABCs are expanded in a mouse model of rheumatoid arthritis (5). There is an acute increase of ABCs induced by viral infection in non-autoimmune mice (6). In a similar manner, there are numerous examples of ABCs in the context of autoimmune disease in humans. While present at low frequency in the peripheral blood of healthy individuals, ABCs are expanded in aged individuals (especially females), in patients with chronic viral infection, and in individuals with several autoimmune diseases including Systemic Lupus Erythematosus (SLE), Rheumatoid Arthritis (RA), and multiple sclerosis (MS) and in common variable immunodeficiency (CVID) [review in (7)].

Transcriptional profiling of ABCs suggests that they have a memory-like phenotypes, such as increased proportion of IgD-/IgM-, and high expression of activation markers such as CD80 and CD86 (2). They also express high levels of CXCR6 and CXCR3, which are involved in homing to sites of inflammation (8, 9). Studies from SLE patients suggest ABCs are precursors of autoantibody-producing plasma cells. IgD-/CD27-, double-negative 2 (DN2) or CD11c+T-bet+ B cells can differentiate into Ig-secreting plasma cells in ex vivo stimulation conditions that include stimulation with a TLR7 agonist or IL-21 (1, 10). Murine CD11c+ B cells, which were identified by the Marrack and Cancro laboratories, have many similarities to CD11c+ atypical memory B cells in humans (2, 11); Like human ABCs, murine CD11c+ B cells express T-bet and activation markers. ABCs are hyporesponsive to stimulation through the B cell receptor (BCR) and CD40 but are responsive to toll-like receptor (TLR) 7/9 stimulation and produce autoantibodies and cytokines, such as IL-4 and IL-10 (11). In the acute LCMV infection model, T-bet+CD11c+ ABCs can produce high amounts of anti-viral antibody following ex vivo stimulation with a TLR7 agonist (12). In that study, most ABCs developed independent of a germinal center (GC) response. In autoimmune mice, ABCs produce more antichromatin IgG2a than non-ABCs (3). The importance of TLR7 signaling in the production of autoantibodies in lupus-prone mice is demonstrated by the autoantibody production that occurs with TLR7 inhibition (13). ABCs can form stable interaction with T cells and act as antigen presenting cells (APCs) (14). They reside at the T/B border in the spleen which increases interactions with T cells. Their localization is partly due to an increased expression of CCR7 and decreased expression of CXCR5. It has been shown that ABCs contribute to

the aberrant differentiation of T follicular helper (Tfh) cells leading to dysregulation of an antigen-specific GC response (15). The pathogenic role of CD11c+ ABCs in autoimmune disease is also evident from studies showing that the removal of these cells significantly ameliorates disease severity and disease progression in the SHIP-deficient B cell mouse model of lupus (15).

Distinct metabolic pathways are required for the specific functions of cells, and modulation of cellular metabolism may normalize cell-specific pathogenic function in disease conditions. Here, we investigated the cellular and molecular mechanisms of ABCs as APCs in Sle1/2/3 triple congenic (TC), a mouse model of SLE. Transcriptome analyses suggested that ABCs have increased expression of molecules involved in antigen uptake, cytokine signaling, and metabolism. ABCs exhibit increased expression of activation markers and a distinct cytokine profile. They express several receptors which are involved in phagocytosis and they uptake a higher amount of soluble antigen than non-ABCs. ABCs induce strong T cell activation and differentiation skewed toward IL-21 producing Tfh cells. They display more active mitochondrial metabolism and reactive oxygen species (ROS) production than FO B cells. Blocking mitochondrial metabolism and mitochondrial ROS production by metformin prevents their ability to induce Tfh differentiation, in part through an inhibition of antigen uptake.

## Materials and methods

### Mice

C57BL/6J, B6; NZM-Sle1<sup>NZM2410/Aeg</sup> Sle2<sup>NZM2410/Aeg</sup> Sle3<sup>NZM2410/Aeg</sup>/LmoJ (stock number 007228) triple congenic (TC) mice, B6.lpr (stock number 000482) (16), C57BL/6J (stock number 000664) and C57BL/6-Tg(Nr4a1-EGFP/cre) (Nur77-GFP, stock number 016617) (17) were purchased from the Jackson Laboratory (Bar Harbor, ME) and bred in house. OT II. Nur77-GFP mice were generated by breeding Nur77-GFP and OT II (B6.Cg-Tg (TcraTcrb425Cbn/J, stock number 004194) and maintained at the FIMR. Female mice were used for all experiments. ABCs and FO B cells were isolated and characterized from 8–10-month-old mice, and 6–8 weeks old mice were used to isolate naïve T cells. We confirmed the disease status by measuring anti-dsDNA IgG and proteinuria. TC and B6.lpr mice were positive for both anti-dsDNA IgG and proteinuria, compared with age matched C57BL/6J mice. Mice were housed at the center for Comparative Medicine at the FIMR with standard 12 hours light/darkness cycle, ambient temperature 23 °C and were provided rodent diet (Lab Diet, St. Louis, MO) and water ad libitum.

### Metformin treatment and immunization

To examine the effect of metformin on ABCs in TC mice, metformin (2.5 mg per mouse) or saline was administered i.p. daily for 1 week. To induce GC B cells, C57BL/6J mice were immunized with NP-CGG (100 µg) in alum intraperitoneally.

## Phenotyping and isolation of cells by flow cytometry

Single cell suspension was prepared from the spleen using a stand protocol. After removing red blood cells (RBC) by RBC lysis buffer (ThermoFisher Scientific, cat no. 00-4333-57, Waltham, MA), the cell suspension was filtered through 70  $\mu\text{m}$  filter. Cell counts were obtained on Cellometer auto 2000 cell counter (Nexcelome, Lawrence, MA) using acridine orange to discriminate nucleated cells from debris and propidium iodide to discriminate dead cells. For immune cell phenotyping, live cells were identified by exclusion of live/dead cell dye (fixable viability dye eFluor506, Invitrogen) positive cells, and were stained on EasySep buffer [HBSS 1x supplemented with 0.5 M EDTA and 2% heat-inactivated fetal bovine serum (FBS)]. For surface staining, single cell suspension was prepared and washed with EasySep buffer.  $1.5 \times 10^6$  cells were incubated with antibody cocktail for 20 min on ice in dark and washed with 10 volumes of EasySep buffer three times. Intracellular staining was performed with True Nuclear staining kit (Biolegend) followed manufacture's protocol. After completion of surface staining, cells were fixed with fixation solution for 45 min at room temperature in dark. Fixation solution was washed with 1x Perm solution twice, and antibodies for intracellular staining (in Perm solution) was incubated for 45 min at room temperature in dark. Flow cytometry was performed on BD FACS Symphony A3 (BD Biosciences) for analysis or BD FACSAria IIu (BD Biosciences) for sorting.

Antibodies were purchased from company and company name and clone number are indicated as followed: anti-CD11c (BD Pharmingen, clone# N418), anti-CD93 (eBioscience, clone# AA4.1), anti-CD95 (BD Bioscience, clone# Jo2), anti-GL7 (eBioscience, clone# GL-7), CD21/CD35 (Biolegend, clone# 7E9), anti-B220 (BD Bioscience, clone# RA3-6B2), anti-CD19 (BD Pharmingen, clone# 1D3), anti-CD23 (Biolegend, clone# B3B4), purified rat anti-mouse CXCR5 (BD Pharmingen, cat# 551961), goat-anti-rat IgG (H+L)-Biotin (Southern biotech, cat#3030-08), anti-TCR $\beta$  (Biolegend, clone# H57-597), anti-CD4 (Biolegend, clone# GK1.5), anti-PD-1 (BD Bioscience, clone# J43), anti-CD44 (BD Bioscience, clone# IM7), anti-CD62L (BD Bioscience, clone# MEL-14), anti-CD11b (Biolegend, clone# M1/70), anti-MHC II (eBioscience, clone# M5/114.15.2), anti-CD36 (eBioscience, clone# HM36), anti-CD86 (eBioscience, clone# GL1), anti-SLAM (Biolegend, clone# TC15-12F12.2), anti-ICOS-L (eBioscience, clone# HK5.3), anti-IgD (BD Bioscience, clone# 11-26c-2a), anti-IgM (eBioscience, cat# 11/41), anti-T-Bet (Biolegend, clone# 4B10), anti-IgG1 (BD Pharmingen, clone# A85-1), anti-IgG2a/2b (BD Pharmingen, clone# R2-40), anti-IgG3 (BD Pharmingen, clone# R40-82), anti-IgA (eBioscience, clone# mA-6E1), anti-Ki67 (BD Bioscience, clone# B56), anti-BCL6 (eBioscience, clone# BCL-DWN), anti-IL-17 (eBioscience, clone# eBio1787), anti-IFN $\gamma$  (eBioscience, clone# XMG1.2), and anti-IL-4 (Biolegend, clone# 11B11). Intracellular IL-21 was detected by IL-21 R-Fc (R&D System) followed by AF488-cojugated goat anti-human IgG (Jackson Laboratory).

## Quantification of OVA uptake by flow cytometry and Image stream

ABCs or FO B cells were incubated alone or with 10  $\mu\text{g}/\text{ml}$  FITC-OVA (Invitrogen) or DQ-OVA (Invitrogen) for 30 min at 37°C for internalization. OVA uptake by B cell subsets was measured by incubation of splenocytes with 10  $\mu\text{g}/\text{ml}$  of OVA-AF488 or OVA PE-TR (both were purchased from Invitrogen) for 30 min at 37 °C. After incubation, free OVA was removed by washing with ice-cold staining buffer and B cell subsets were identified by staining for surface markers. To block the CD36, 10  $\mu\text{g}/\text{ml}$  of control IgA (Abcam, S107, ab37322) or anti-CD36 neutralizing antibodies (Cayman, clone: JC63.1) were treated with B cells for 2 hours before OVA incubation. After the incubation, cells were washed with ice-cold staining buffer three times and resuspend in PBS at  $10^6/\text{ml}$  concentration. Percent of OVA positive B cells and intensity of OVA in B cells were quantified by flow cytometry analysis. Internalized OVA was identified by Imaging flow cytometry. Imaging flow cytometry was performed on an ImageStreamX Mark II. 1000 of CD19+ single live B cells were acquired for the analysis in each sample.

## *In vitro* differentiation of Tfh by B cells and metformin treatment

ABCs and FO B cells were purified from spleens by cell sorter and plated into round bottom 96 well plate ( $10^5$  cells/well). OVA protein (EndoFit OVA was purchased from InvivoGen, cat# vac-pova) was added (10  $\mu\text{g}/\text{ml}$ ) for 3 hours before addition of T cells. Naïve CD4 T cells were isolated from spleens of OT II mice by CD4+ naïve T cell isolation kit from Stem cell technologies (cat# 19765A, Stem cell technology). Purity of naïve CD4+ T cells was confirmed by flow cytometry and average 95% purity was obtained. Isolated naïve CD4+ T cells were added to the B cell culture at the ratio of 2:1 (B cells: T cells) in total 200  $\mu\text{l}$ . Cells were incubated at 37 °C, CO<sub>2</sub> (5%) incubator for 3-4 days. For metformin inhibition assay, isolated B cells were incubated with 1 mM metformin (item no. 13118, Cayman chemical) or phenformin (item no. 14997, Cayman chemical) for 2-3 hours and cells were washed with media 3 times to remove free metformin in the following culture.

## Cytokine measurement

Secreted cytokines from B cells were measured by either mouse proinflammatory panel 1 from mesoscale discovery (MSD, cat# N05048A-1) followed by manufacture's protocol. All the samples were measured in duplicates, and any value within the linear range of each cytokine was taken as data.

Intracellular cytokine production was measured by flow cytometry. Briefly, cells were stimulated with PMA (100 ng/ml) and ionomycin (1  $\mu\text{g}/\text{ml}$ ) for 6 hours on the day of assay. To accumulate the cytokine inside of cells, BFA (20  $\mu\text{g}/\text{ml}$ ) was added

during the last 4 hours of stimulation. Staining procedure for intracellular staining and surface staining are followed as described in previous section. Frequency of each cytokine positive cells was calculated after exclusion of dead cells.

## Lactate/ATP measurement

B cells were isolated and cultured overnight. Next day, intracellular ATP level was measured from cell pellet by Luminescent ATP measure kit (Abcam) and culture supernatant was collected for lactate assay by Lactate colorimetric/fluorometric assay kit followed by manufacturer's protocol (BioVision). Luminescence of ATP assay was measured by Victor 1420 (Perkin Elmer) and lactate assay absorbance (OD570 nm) was measured by Synergy H1 microplate reader (BioTek).

## Intracellular metabolism assay

For mitochondria contents and membrane potential, cells were incubated with MitoTracker red (Invitrogen, cat# M22425) and MitoTracker green (Invitrogen, cat# M7514) at a concentration of 10 nM in complete media for 15 min at 37°C. To measure of glucose uptake, cells were incubated with 100  $\mu$ M 2-NBDG (Cayman, cat# 11046) for 20 min at 37°C in complete media. Cellular ROS was measured by MitoSOX (1  $\mu$ M) or H2DCFDA (1  $\mu$ M). Cells were incubated in 500  $\mu$ l of MitoSOX or H2DCFDA for 10 min at 37°C. After the labeling, cells were washed three times with staining buffer and analyzed by flow cytometry.

## Seahorse experiments

A Seahorse XFp Extracellular Flux Analyzer was used to measure OCR and ECAR of ABC and FO B cells using the MitoStress test condition by Agilent seahorse. ABC and FO B cells were immobilized to create a monolayer of cells ( $2 \times 10^5$ ) on XFp microplates using the manufacturer protocol for immobilization of non-adherent cell using Cell-Tak (Corning). Assay medium was made by using XFp Base medium enriched with 2.5 M of Glucose, 100 mM of pyruvate and 200 mM Glutamine per 10 mL of XFp base Medium all from Agilent seahorse. Baseline and maximal ECAR and OCR values were averaged between 3 replicates per sample for 3 successive time intervals.

## RNA purification and RT-qPCR

Total RNA was purified from sorted cells by Direct-zol RNA MicroPrep (ZymoResearch). Genomic DNA was removed by in-column DNA digestion during the RNA preparation. 200 ng of isolated RNA was converted to cDNA by iScript DNA synthesis kit (BioRAD) and quantitative PCR was performed as previously described (18). Primers were purchased from ThermoFisher as follows: *Polr2a* (Mm00839503\_m1), *Il12a* (Mm00434169\_m1), *Il1b*

(Mm00434228\_m1), *Tnf* (Mm00443258\_m1), *Il6* (Mm00446190\_m1), *Il10* (Mm01288386\_m1), *Hk2* (Mm00443385\_m1), *Mthfd2* (Mm00485276\_m1), *Slc2a1* (Mm00441480\_m1), *Stat5* (Mm03053818\_s1), *Cd36* (Mm00432403\_m1), *Axl* (Mm00437221\_m1), *Hifa* (Mm00468869\_m1), *Slc22a1* (Mm00456303\_m1), *Slc22a2* (Mm00457295\_m1) and *Slc22a3* (Mm00488294\_m1). The reference gene, *Polr2a*, was used for normalization and relative expression was calculated by  $2^{-\Delta\Delta C_t}$  method.

## Quantification of mitochondria

To isolate mitochondria DNA and genomic DNA, isolated B cells were lysed, and total DNA was isolated by DNeasy gDNA isolation kit (QIAGEN). In-column Rnase treatment was performed to remove RNA contamination. Mitochondrial DNA was quantified by levels of *Nd1* (NADH dehydrogenase subunit 1) and *Rnr2* (16S ribosomal RNA) and nuclear DNA was quantified by level of actin. Primers for qPCR were purchased from Taqman (Invitrogen); Mm04260181\_s1 (*Rnr2*), Mm04225274\_s1 (*Nd1*), and Mm00607939\_s1 (*Actb*). To determine the mitochondrial DNA contents, relative to nuclear DNA calculated using the following equations: a)  $\Delta C_T = (\text{nucDNA } C_T - \text{mtDNA } C_T)$ , b) Relative mitochondrial DNA content =  $2 \times 2^{-\Delta C_T}$ .

## Quantitation of oxidized lipid

Oxidized lipid was detected by labeling of C11-BODIPY (581/591) (catalog number D3861, TermoFisher), an oxidation-sensitive fluorescent probe (19). Isolated B cells were incubated with 5  $\mu$ M of C11 for 30 min at 37°C. Labeled cells were washed with washing buffer three times and fluorescence was analyzed by flow cytometry.

## RNA-Seq and bioinformatics

CD11c+ ABCs and FO B cells were freshly isolated and snap-frozen for further process. RNA purification, library preparation and sequencing were performed by Azenta (AZENTA life sciences). Briefly, total RNA was purified, and mRNA was selected with polyA selection. QC of purified RNA and amplified cDNA were confirmed, and only high quality of samples were used for the sequencing. 2x150 base pair, single index sequencing (paired-end) was performed using an Illumina HiSeq sequencer.

QC for fastq files was performed with FastQC. Reads were mapped to the mouse genome (GRCm39) using STAR2 (20). The aligned reads were quantified with htseq-counts to the M29 annotation. Raw counts were compiled to identify differentially expressed gene and analyzed using DESeq2. Genes were considered differentially expressed if they showed at least 1 absolute log2-fold changes and a false discovery rate of <0.05. Pathway/gene set enrichment was done using fgSEA on MSigDB gene sets (21–23). RNA-Seq data was also analyzed by using the RNA-Seq workflow in Petek Flow software (Partek Inc., St. Louis, MO). Statistical analysis and plotting were performed with R+tidyverse and pheatmap used to draw heatmaps.

## Mass spectrometry-based metabolomic analysis

Sample preparation, process and analysis was followed by previous report with modification (24).  $5 \times 10^5$  ABCs or FO B cells were sorted by cell sorter. Isolated cells were washed with ice-cold HBSS three times and snap-frozen until following steps. Cells were lysed by incubation with extraction solvents (50:50 v/v methanol:acetonitrile) for 1 hour at  $-20^\circ\text{C}$ . Lysed cell extracts were centrifuged and upper layer (containing metabolites) were collected and further processed by LC-tandem mass spectrometry (MS/MS). Chromatography was performed with a Shimadzu Nexera system (Shimadzu, Columbia, MD) coupled with a high-resolution hybrid quadrupole time-of-flight mass spectrometer (TripleTOF 5600, Framingham, MA).

Targeted metabolomic data were processed using Peak View 2.1 and MultiQuanta software version 3.0.2 (SCIEX). Chromatographic peaks of targeted metabolites were annotated, and each identified metabolite was quantified by integrating peak area using MultiQuant software. The quantitative analysis was based on the total peak areas of extracted ion chromatograms of feature ions. Principal component analysis plot and heat map were generated with MetaboAnalyst (v4.1).

## Statistics

Statistical analyses and significance were performed using GraphPad Prism v.9.02 software (GraphPad Software Inc.). Nonparametric student-test, either Mann-Whitney test or Wilcoxon matched-pair test, or one-way ANOVA with Sidak's correction for multiple comparisons. All the data are reported as mean.

## Study approval

All animal experiments and procedures were performed according to protocols approved by the Institutional Animal Care and Use committee at the Feinstein Institutes for Medical Research (FIMR) (approved protocol no. 2022-022 term I).

## Results

### CD11c+ ABCs are T-bet positive and exhibit features of professional antigen presenting cells

ABCs are defined differently across studies. CD21-CD23- B cells are a heterogeneous population that includes CD11c+ B cells. We investigated the T-bet expression in B cell subsets since T-bet expression is one of the markers of human circulating ABCs (25). T-bet expression was not observed in conventional B2 B cells (FO and marginal zone) but most CD11c+ CD21-, CD23- B cells express

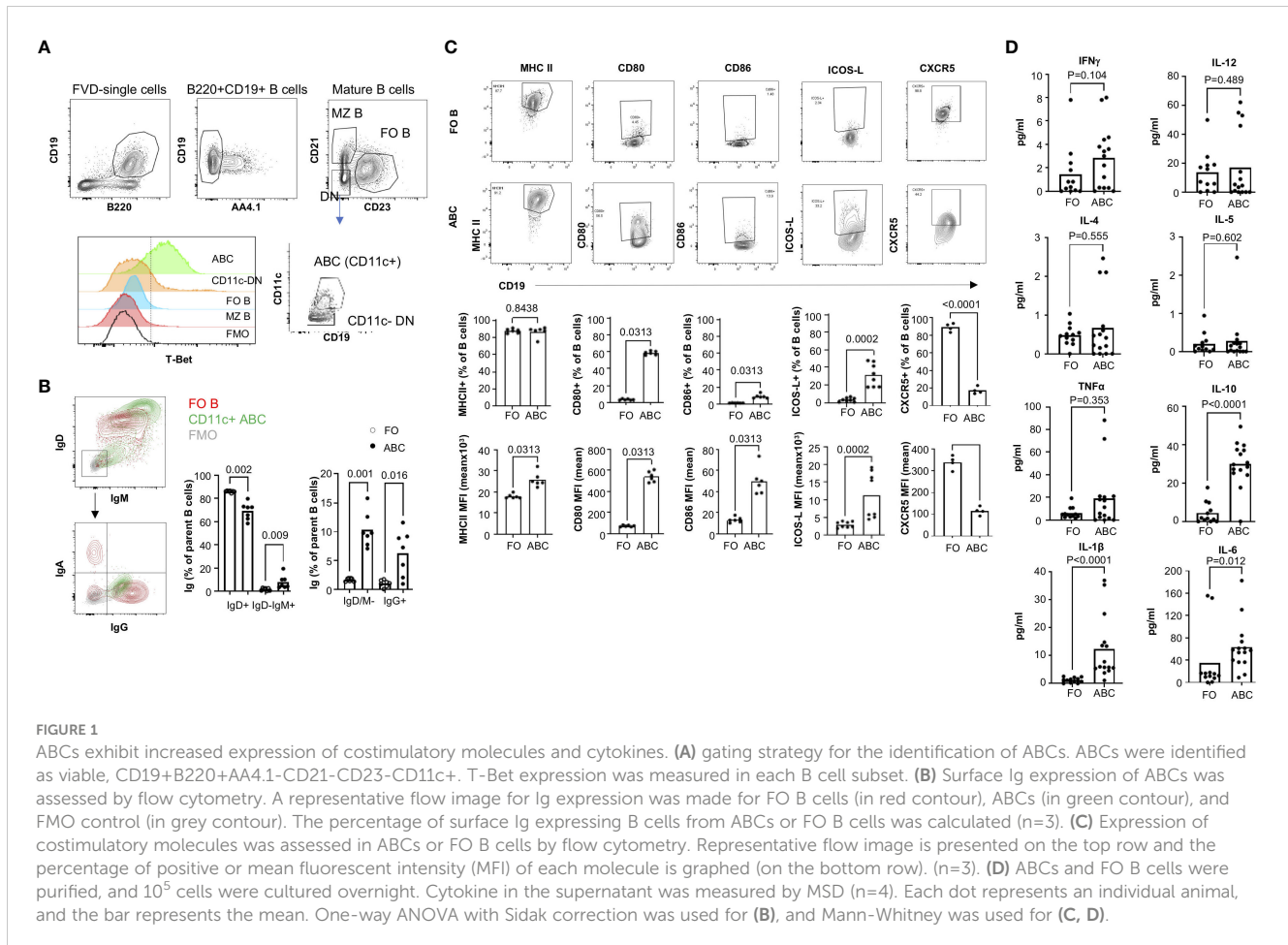
T-bet (Figure 1A). There are few T-bet+ cells detected in CD11c-CD21-, CD23- B cells (Figure 1A). Therefore, we defined CD11c+, T-bet+, CD21-, and CD23- B cells as murine ABCs and focused on this population for the current study. In human, ABCs have memory-like phenotypes with IgG expression (1). We wanted to know whether ABCs are class-switched in TC mice, and ABCs display isotype heterogeneity; the majority of ABCs are IgD<sup>hi</sup>/IgM+, and there are few IgD-/IgM- cells, which are IgG+. The frequency of class-switched B cells is higher in ABCs than FO B cells (Figure 1B). Since the majority of ABCs are IgD<sup>hi</sup>/IgM+ (70%), we decided to compare ABCs to FO B cells.

ABCs are known to express an increased level of MHC II and co-stimulatory molecules compared to FO B cells in aged female mice (2), and we confirmed the higher expression of CD80, CD86 and MHC II in ABCs (Figure 1C). We also observed ICOS-L expression, which delivers a positive signal for Tfh differentiation, in ABCs and not in FO B cells. CXCR5 expression on ABCs is a topic of debate (11, 14). We found ABCs express much lower levels of CXCR5 than FO B cells (Figure 1C).

In addition to differences in expression of co-stimulatory molecules, cytokine production by ABCs was distinct that observed in FO B cells. We measured cytokines in the supernatant from isolated ABCs or FO B cells. There are reports that secretion of TNF $\alpha$ , IL-4 and IL-10 from ABCs in aged mice (11, 26). We observed increased IL-10 but not TNF $\alpha$  or IL-4 in ABCs compared to FO B cells from TC mice. We also did not find an increased production of Th1 type inflammatory cytokines, IFN $\gamma$  or IL-12, in the supernatants of ABCs although both are positively regulated by T-bet in T cells. Instead, IL-1 $\beta$  and IL-6 were highly produced by ABCs compared to FO B cells (Figure 1D). These data suggest that ABCs are activated B cells, have a distinct cytokine profile, and may induce T cell activation/differentiation more efficiently than FO B cells in TC mice.

### Distinct transcription profile in pathways related to antigen presentation, phagocytosis and metabolism in ABCs

To understand further the functional difference between FO B and ABCs, we compared their transcriptomic profiles. FO B cells and ABCs were purified and bulk RNA-Seq analysis was performed. Principal component analysis (PCA) analysis revealed a clear separation between FO B cells and ABCs (Figure 2A). The volcano plot showed that 1716 genes are up-regulated, and 1595 genes are down-regulated in ABCs compared to FO B cells (log2-fold change  $>1$  or  $<-1$ , adj p-value  $<0.05$ ) (Figure 2B). Pathway analysis was performed by fgSEA using MsigDB's hallmark set. Genes involved in membrane invagination (Supplementary Figure 1) and phagocytosis (data not shown) were differentially expressed in ABCs compared to FO B cells, as were genes involved in apoptosis, cytokine signaling (TNF $\alpha$ , and IL-2/STAT5) and metabolism (mTORC1, glycolysis, and hypoxia) (Figures 2C, D). Selected RNA-Seq data were confirmed by qRT-PCR in a separate



cohort (Figure 2E). Gene expression data suggest that ABCs are more effective antigen presenting cells with phagocytic activity. They also have a distinct metabolic program, characterized by increased glycolysis and a hypoxia response, and an increased proinflammatory cytokine/cytokine signaling compared to FO B cells.

## Increased antigen uptake by ABCs

The frequency of B cells recognizing a specific antigen is very low, usually less than 0.05% in the normal repertoire (27). Enrichment of genes involved in phagocytosis, autophagy, and membrane invagination led us to investigate whether ABCs have antigen uptake mechanisms other than the BCR-dependent mechanism. Innate immune cells uptake soluble antigens through antigen independent mechanisms including phagocytosis, Fc-dependent endocytosis, and pinocytosis [reviewed in (28, 29)], but B cells, in general, internalize antigens through a direct interaction between the antigen and the BCR. We asked whether a high percent of ABC would uptake a particular antigen, ovalbumin (OVA). Each B cell subset was incubated with FITC-OVA [ $\sim$  3 nm hydrodynamic size (30)], and OVA+ B cells were

enumerated. B cells were also incubated with DQ-OVA which enabled us to identify OVA in the lysosome to assess peptide processing of the ingested OVA protein in B cells. Approximately 25% and 15% of ABCs were positive for FITA-OVA or DQ-OVA, respectively compared to less than 5% of FO B cells (Figure 3A). We confirmed the intracellular location of OVA by image stream (Figure 3B). Then, we assessed uptake of another antigen, FITC-Dextran (1 nm diameter) by ABCs. Classical dendritic cells (cDCs: lin-CD11c<sup>hi</sup>B220-MHCII<sup>hi</sup>) were included as a positive control for phagocytic activity, approximately 40% of cDCs ingested FITC-Dextran. We detected FITC-Dextran in approximately 20% of ABCs and less than 5% of FO B cells (Figure 3C). Uptake of FITC-Dextran or FITC-OVA did not occur when cells were incubated on ice confirming that positivity did not represent membrane binding. Both OVA and Dextran are small molecules that can be ingested by pinocytosis. To address whether OVA uptake and T cell activation is ABC lineage-specific or results from inflammatory conditions in lupus mice, we investigated OVA uptake by ABCs from aged female C57BL/6J mice. A significant amount of OVA was ingested by ABCs from non-lupus mice (Supplementary Figure 2A). However, we did not detect T cell activation or Tfh differentiation by OVA+ABCs from non-autoimmune mice (Supplementary Figure 2B).

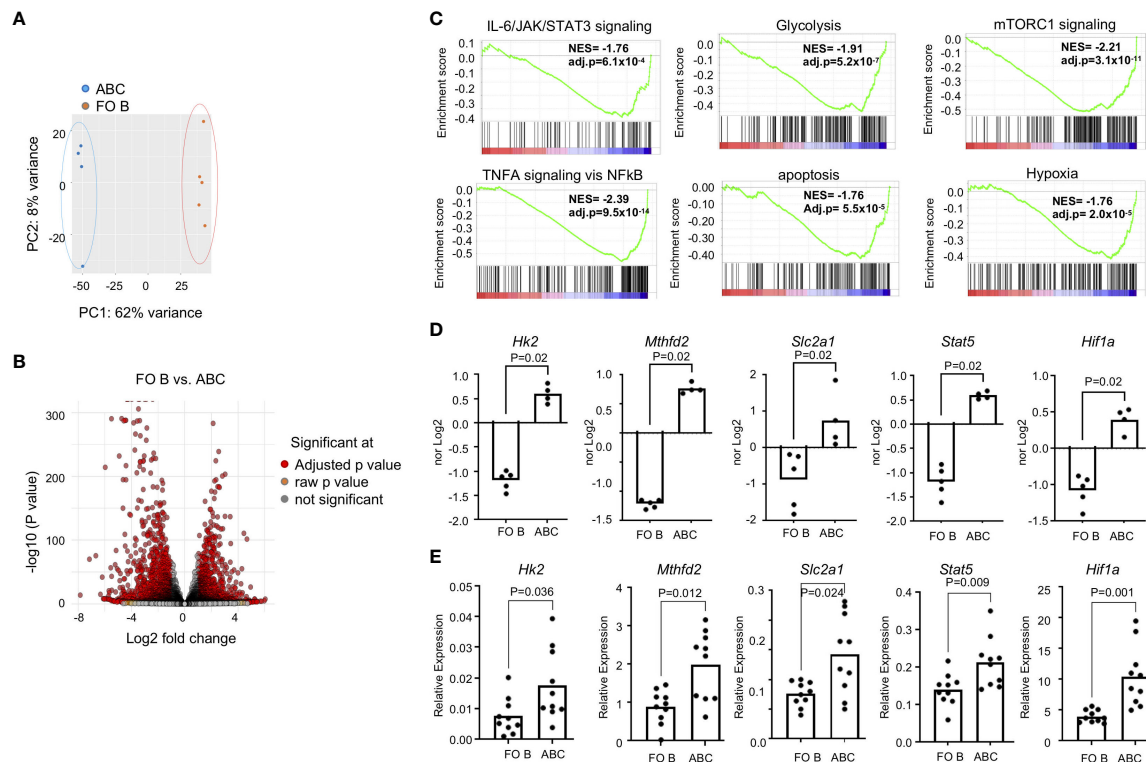


FIGURE 2

ABCs have a distinct transcription identity. ABCs and FO B cells were isolated, and transcriptome was assessed by RNA-Seq. (A) PCA was performed and first and second principal components are plotted. (B) Volcano plot was made from the data. (C) Gene set enrichment analysis was made from the gene expression data set from B and enrichment score was plotted. (D) Normalized expression was plotted from the gene expression data from (B, E) Gene expression was performed by qRT-PCR in a separate cohort. Relative expression of each gene of interest was calculated as a relative expression of reference gene, *Polr2a*. ( $n=3$ ). Each dot represents an individual mouse, and the bar represents the mean. Unpaired Mann-Whitney was used for statistical test.

The differentially expressed genes seen by RNA-Seq suggest several phagocytic receptors may be expressed in ABCs. We confirmed the expression of CD36 by qRT-PCR and surface expression of CD36 by flow cytometry (Supplementary Figure 3A, B). Expression of CD36 suggests that ABCs might internalize antigens by phagocytosis. We, therefore, asked whether CD36 expression is required for OVA uptake by ABCs. Co-staining with CD36 and OVA-FITC showed that OVA was taken up in both CD36+ and CD36- ABCs (Supplementary Figure 3C). Moreover, blocking CD36 by neutralizing antibodies did not affect OVA uptake (Supplementary Figure 3D). We also tested whether ABCs were able to phagocytose a large particle (typically 1–2  $\mu\text{m}$ ), Zymosan. Less than 5% of ABCs exhibited phagocytic activity (data not shown). These data suggest that ABCs can uptake small antigens by a non-phagocytic mechanism, and CD36 does not participate in this process.

Since ABCs exhibit phenotypes of activated B cells, we compared ABCs with GC B cells which are antigen activated B cells. GC B cells (CD95+GL7+) express high levels of MHC II and CD86 but not CD80 (Figure 4A). Cytokine expression from FO B, GC B, and ABCs showed more significant difference between GC B and ABCs as shown in Figure 4B. Similar to FO B cells, GC B cells showed little expression of proinflammatory cytokines (*Il1b*, *Il6* and *Ifng*). Both ABCs and GC B cells have an increased expression of

genes involved in glycolysis and *Stat5* compared to FO B cells, but *Hif1a* expression was increased only in ABCs. Lastly, we compared OVA uptake and GC B cells that show low OVA uptake compared to ABCs (Figure 4C).

## ABCs induce stronger T cell activation and promote Tfh differentiation

Next, we wanted to address whether ABCs play a role in T cell activation as APCs. First, we asked if the ABCs can activate T cells through the T cell receptor (TCR). We compared Nur77 induction in T cells, an immediate downstream molecule in TCR signaling. The expression of Nur77 is positively correlated with TCR strength and is not induced by non-TCR signaling such as signaling through cytokine receptors (17, 31). Naïve CD4+ T cells from OTII.Nur77-GFP mice were cultured with ABCs or FO B cells, pre-incubated with or without OVA protein. ABCs induced a stronger TCR signal, assessed by expression of Nur77-GFP in naive CD4 T cells (Figure 5A) and T cell activation was OVA dependent, as there was minimal Nur77 induction by ABCs in the absence of OVA.

Next, we assessed T cell proliferation/activation induced by ABCs or FO B cells. After 3 days of co-culture, there were more live T cells in the culture containing ABCs with OVA than FO B cells

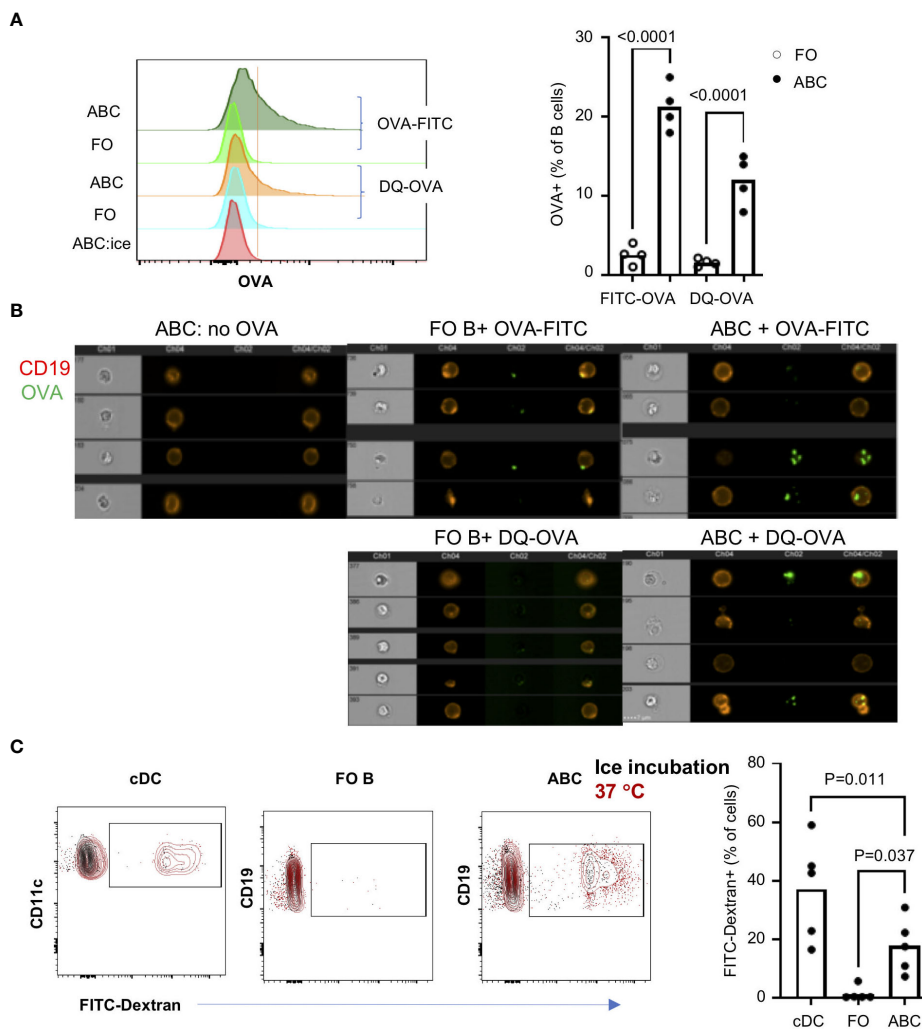


FIGURE 3

ABCs not FO B cells uptake soluble antigens. ABCs and FO B cells were isolated and incubated alone or with 10  $\mu\text{g/ml}$  of OVA-FITC or DQ-OVA for 30 min at 37°C. To exclude the non-specific binding of OVA, ABCs were incubated with OVA-FITC on ice for 30 min (ABC:ice). After the incubation, OVA signal was detected and analyzed by flow cytometry or image stream. (A) A representative overlaid histogram image from the flow cytometry analysis is on the left side and the percent of OVA-positive cells is plotted on the right side. Each dot represents an individual mouse (value was an average of technical duplicates) (n=4). (B) OVA location was analyzed by image stream. 4 representative images from each condition are presented. (C) FITC-Dextran (10  $\mu\text{g/ml}$ ) were incubated with splenocytes for 30 min at 37°C or on ice. After incubation, cells were stained with cell lineage surface markers, and the percent of FITC-Dextran positive cells was analyzed by flow cytometry. Each dot represents individual mouse (value was an average of technical duplicates) and the bar represents the mean (n=2). One-way ANOVA was used for statistics and Bonferroni correction was applied for multiple comparison.

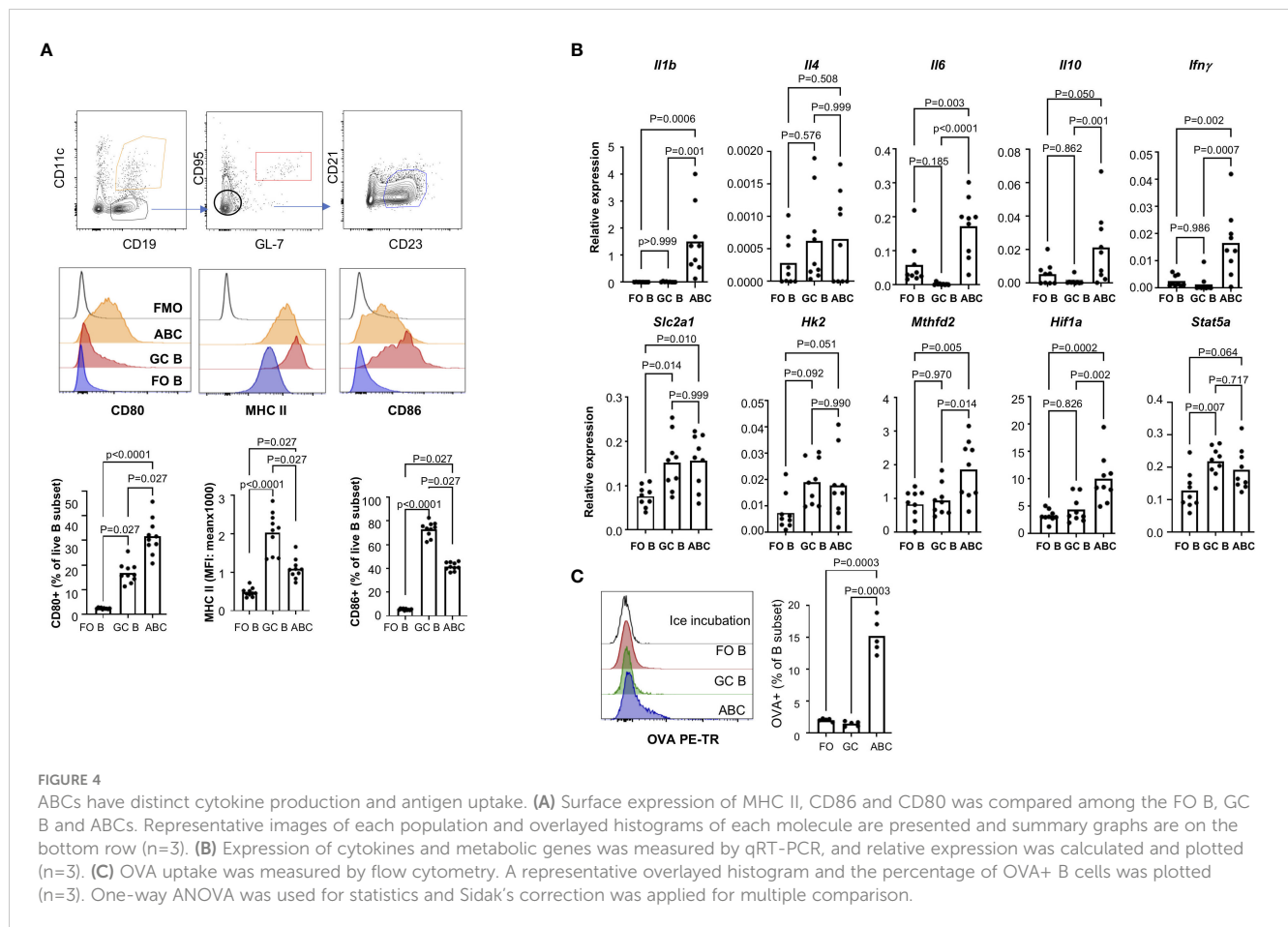
with OVA (Figure 5B). Both FO B cells and ABCs induced Ki67 expression in live CD4+ OTII T cells in the presence of OVA protein (Figure 5C). Although there was no difference in the frequency of Ki67+ T cells, an increased number of CD44+ T cells was observed by co-culture with ABCs (Figure 5D). Next, we compared effector T (Teff) differentiation by OVA-presenting ABCs or FO B cells. ABCs induced little Th1, Th2 or Th17 differentiation and no difference was observed between ABCs and FO B cells (Figure 5E). In contrast, ABCs induced more IL-21-positive T cells than FO B cells (Figure 5E). IL-21 is a key cytokine of Tfh (32). PD-1, CXCR5 (a surface marker of Tfh) and BCL6 (a master transcription factor of Tfh) expression were measured in T cells activated by ABCs or FO B cells to confirm that IL-21 producing T

cells were Tfh; CXCR5+/PD-1+/BCL6+/IL-21+ cells were induced by ABC/OVA-primed T cells but not by FO B OVA-primed T cells (Figure 5F). These data suggest that ABCs can promote preferential differentiation of naïve T cells to Tfh and cognate antigen presentation by ABCs is required.

### ABCs exhibit increased glycolysis, mitochondrial respiration and ROS production

In addition to the enrichment of antigen presentation and phagocytic markers, ABCs display a significant difference in



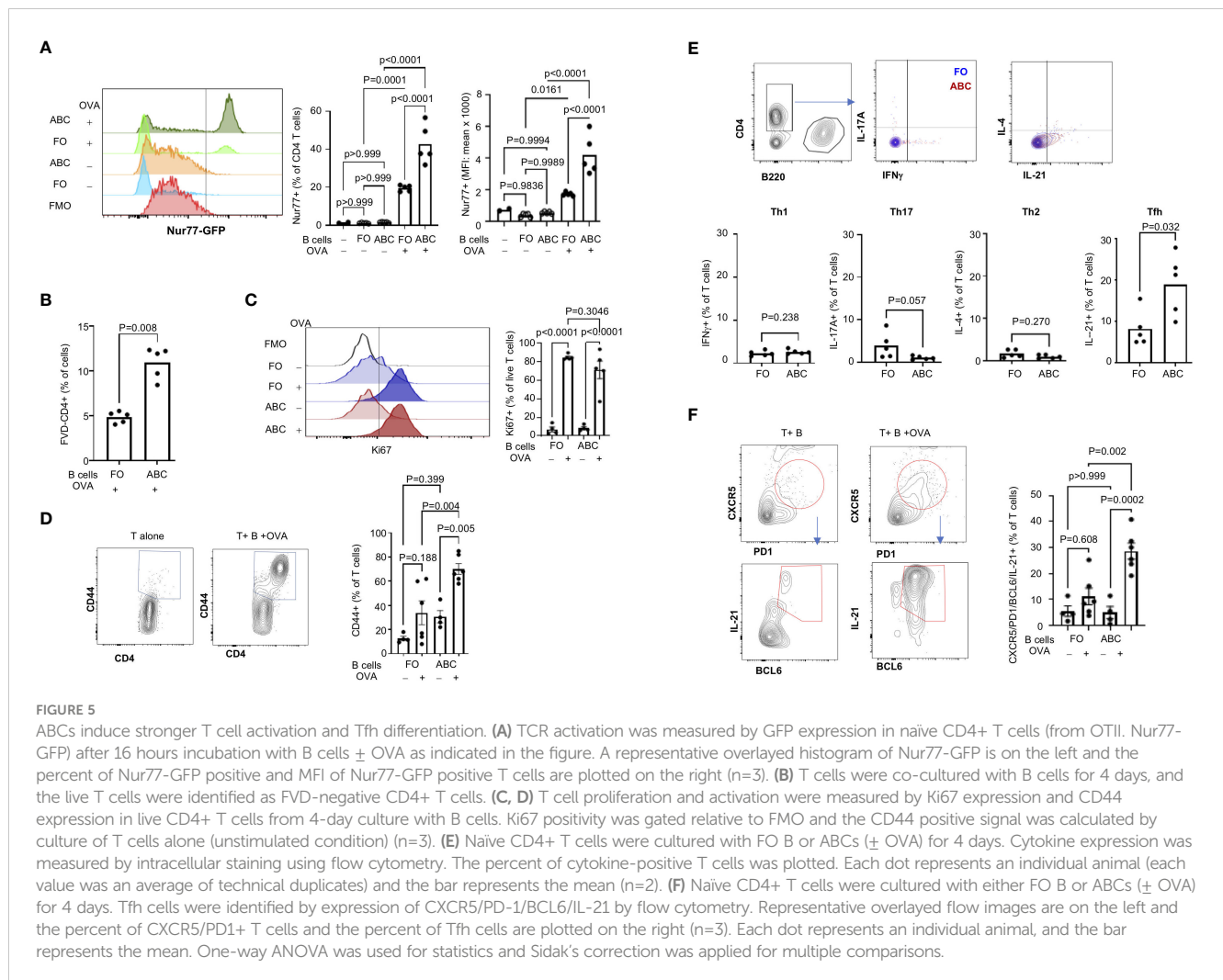


metabolism (in Figure 2). To confirm increased energy metabolism in ABCs, we measured glucose uptake and mitochondrial metabolism. 2-NBDG (2-[N-(7-nitrobenz-2-oxa-1,3-diazol-4-yl)amino]-2-deoxy-D-glucose) is a fluorescent analogue of D-glucose which enables the measurement of glucose uptake in a quantitative manner (33). Consistent with the increased level of *Slc2a1* (the gene encoding Glut1) seen in the RNA-Seq analysis, we found that significantly more 2-NBDG was taken up by ABCs than FO B cells (Figure 6A). Mitochondrial mass and mitochondrial membrane potential were measured by MitoTracker Green and MitoTracker Red, respectively. ABCs exhibited slightly increased mitochondrial mass compared to FO B cells and displayed enhanced mitochondrial membrane potential. Increased mitochondrial mass was confirmed by measuring the mitochondrial genes, *Nd1* and *Rnr2* (Supplementary Figure 4A). Moreover, ABCs exhibited higher levels of reactive oxygen species (ROS) measured by MitoSOX and H2DCFDA (Figure 6A), causing an increased lipid peroxidation in ABCs (Supplementary Figure 4B). Stimulation of B cells either by antigen (anti-IgM) or a TLR7 agonist (R848) increased glucose uptake and cellular ROS production in both B cell subsets (Supplementary Figure 5A). We repeated the experiment in B6.lpr mice, another lupus-prone strain, and observed increased metabolic activity in ABCs compared to FO B cells (Supplementary Figure 5B). An increased mitochondrial

ROS was observed in ABCs, but glucose uptake and mitochondrial membrane potential were not different between unstimulated ABCs and unstimulated FO B cells in aged female non-autoimmune mice (Supplementary Figure 5C). These data suggest a metabolic difference (increased glycolysis, mitochondrial membrane potential and ROS production) in ABCs could be driven by the autoimmune background.

We confirmed the data obtained through flow cytometry analysis by seahorse technology, which allows for simultaneous kinetic measurement of cellular respiration and glycolysis. ABCs from TC mice showed increased oxygen consumption rate (OCR) and extracellular acidification rate (ECAR) at basal state and at the point of maximal respiration compared to FO B cells (Figure 6B). Increased glycolysis in ABCs was confirmed by increased lactate production, which is a final product of glycolysis (Figure 6C).

We further characterized the metabolites in the ABCs and FO B cells using LC-MS/MS analysis. An equal number of ABCs and FO B cells were isolated, and an untargeted metabolome analysis was performed. PCA analysis was carried out using an unsupervised dimensionality reduction method. There was a clear spatial separation between the two groups (Supplementary Figure 6). Fold change and t-test were combined to screen for significantly different metabolites between the groups. Those with a p-value of less than 0.05 and  $\log_2(\text{FC}) > 1$  were considered statistically

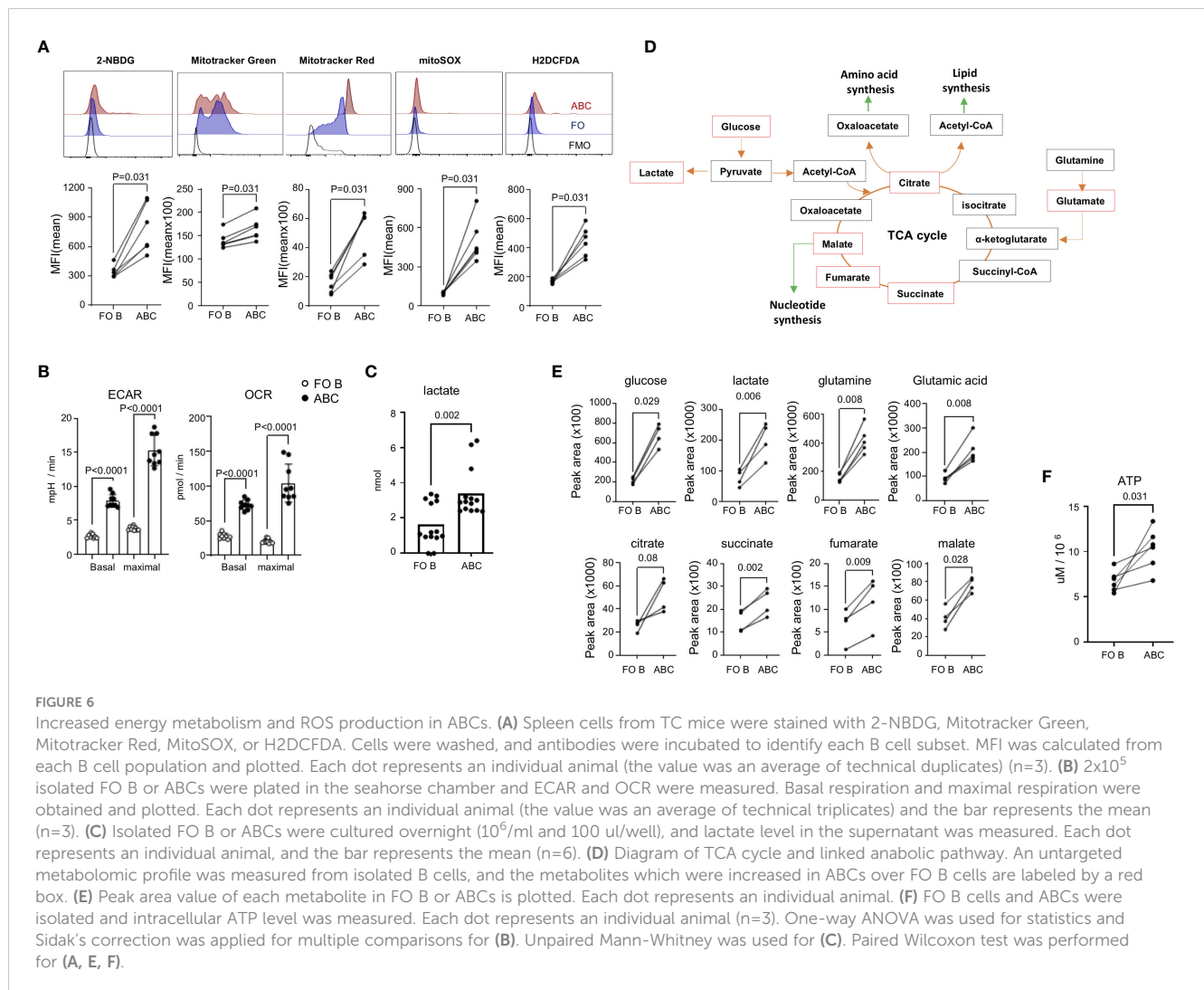


different. The results showed that 87 of 145 metabolites were elevated in ABCs. The heat map of the top 50 differential metabolites is presented in [Supplementary Figure 6](#). Many of these metabolites function within the glycolysis and TCA cycle pathways ([Figures 6D, E](#)). Increased metabolites may result from high energy production or from blocking of a downstream pathway, leading to cell death. To confirm that the increased metabolic status was indeed related to increased energy production in ABCs, we measured the level of intracellular ATP, which was higher in ABCs than FO B cells ([Figure 6F](#)). These data suggest that ABCs are metabolically hyperactivated compared to FO B cells.

## Metformin suppresses antigen uptake and Tfh differentiation by ABCs

Hypermetabolism is closely linked with altered function and differentiation of leukocytes [reviewed in (34)]. Several reports showed that treatment of lupus-prone mice with metabolic modulators can prevent disease development or even reverse the established disease phenotypes (35). Since ABCs display increased

energy metabolism, we wanted to address whether targeting mitochondrial metabolism and ROS production might decrease ABC-mediated Tfh differentiation. Metformin is a drug with pleotropic effects, including inhibition of mitochondrial respiratory chain complex I and production of ROS (36). In B cells, metformin can block terminal differentiation to plasma cells (37), but the effect on ABCs is not known. Because the receptor for metformin in B cells is not known, we measured the expression of metformin receptors in B cells. ABCs express *Slc22a3* but no *Slc22a1* or *Slc22a2* and the level of *Slc22a3* was higher in ABCs compared to FO B cells ([Supplementary Figure 7A](#)). First, we confirmed the effect of metformin on mitochondrial ROS production in B cells; metformin decreased mitochondrial ROS, but not total ROS, in ABCs ([Figure 7A](#)). Next, we determined whether metformin could modulate internalization of FITC-OVA and co-stimulatory molecule expression in ABCs. OVA-positive B cells with or without metformin treatment were quantified by flow cytometry; metformin treated ABCs showed a significant decrease in OVA uptake ([Figure 7B](#)). The inhibition of OVA uptake was also observed when ABCs were treated with phenformin which is a metformin-related drug ([Supplementary Figure 7B](#)), that is transferred into cells in a



non-receptor dependent fashion (38). Metformin treatment did not decrease the surface expression level of MHC II but did decrease CD80 expression in ABCs (Figure 7B). Suppression of OVA uptake and CD80 expression by metformin led us to investigate whether metformin altered T cell activation. It did not lead to decreased T cell viability, but no longer induced Tfh differentiation (Figure 7C). We next investigated the effect of metformin on ABC function *in vivo*. A study by Lee and colleagues showed a significant reduction of most B cell subsets in Roquin<sup>san/san</sup> lupus mice by 3 weeks metformin treatment (37). To avoid the loss of ABCs by long-term treatment with metformin, we treated TC mice with metformin for 1 week, and assessed the function of ABCs. We did not find a significant difference in body weight, number of splenocytes or percentage of B cell subsets in metformin treated TC mice compared to saline treated TC mice (data not shown). We observed a trend of decrease in percentage of ABCs and further decreased OVA uptake observed by ABCs from metformin treated TC mice (Figures 7D, E). The ABCs from metformin-treated TC mice also showed a decreased ability of T cell activation and Tfh differentiation. Overall, these data suggest that metformin treatment inhibits antigen uptake and suppresses Tfh differentiation by ABCs.

## Discussion

Our study shows that ABCs from lupus prone TC mice exhibit a distinct gene expression profile which is specifically enriched in pathways of antigen-uptake, cytokine signaling, and energy metabolism. ABCs engage in active uptake of soluble antigens and express high levels of co-stimulatory molecules for T cell activation, thereby inducing T cell activation skewed toward Tfh differentiation. Moreover, *in vivo* and *in vitro* treatment with metformin decreased antigen uptake by ABCs and subsequent Tfh differentiation.

B cells can contribute to the development of autoimmune disease in various ways. The most prominent way is by the production of self-reactive antibodies which target the host's organs (39). Indeed, several studies have shown that ABCs are able to secrete antibodies after activation. ABCs from lupus-prone mice or virus infected animals produce self-reactive antibodies or anti-viral antibodies, respectively (10, 12). Depletion of ABCs leads to a reduction of autoantibodies in the serum of lupus prone mice (3). Compared to FO B cells, which express low levels of costimulatory molecules, ABCs express costimulatory molecules and higher levels of MHC II. This phenotypic characterization

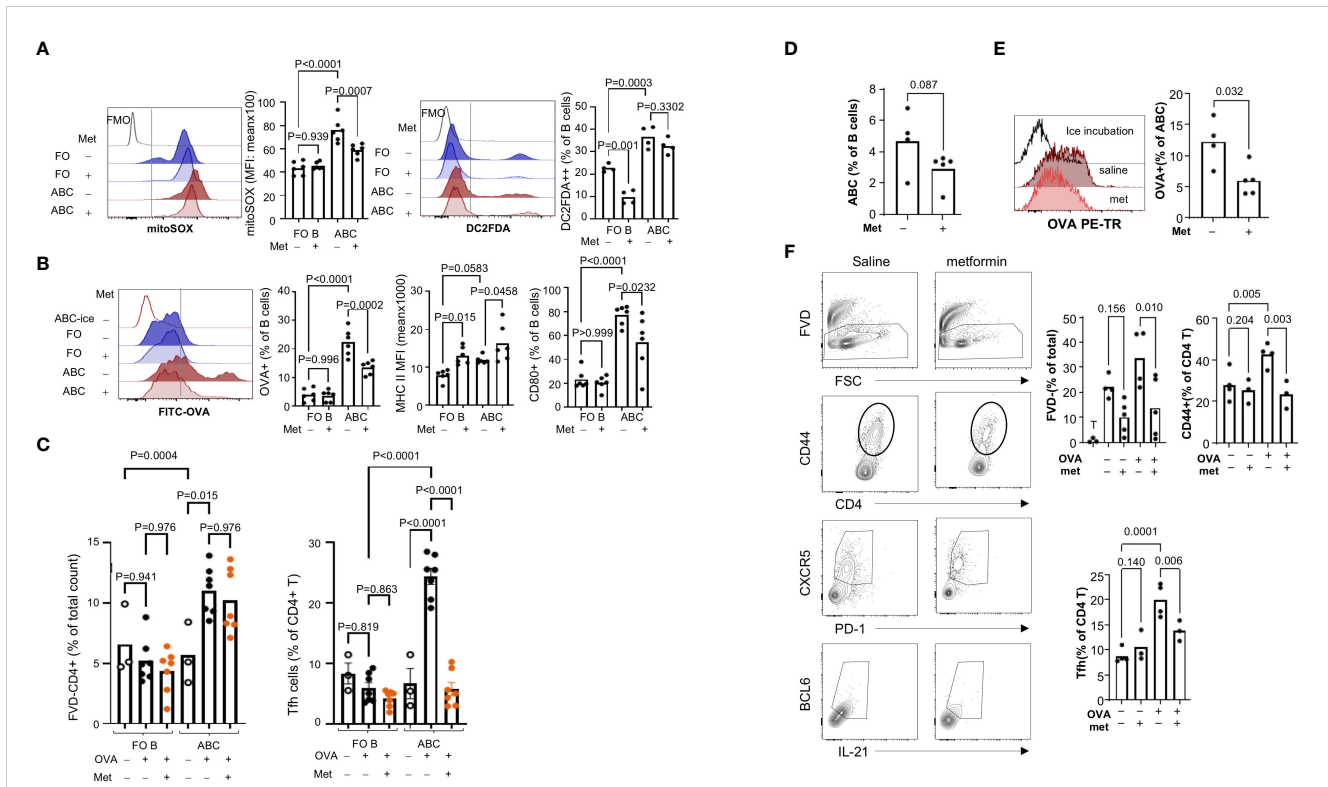


**FIGURE 7**  
 Metformin treatment suppressed OVA uptake by ABCs and subsequent Tfh differentiation. **(A)** ABCs and FO B cells were cultured alone or with metformin (1 mM) overnight. After the culture, mitochondrial ROS production and total ROS production were measured by MitoSOX and H2DCFDA staining. MFI was analyzed by flow cytometry and the value was plotted. Each dot represents an individual animal (value was an average of technical duplicates) and the bar represents the mean (n=4). **(B)** B cells were isolated and cultured alone or with metformin overnight. After the incubation, cells were washed, and incubated with FITC-OVA for 30 min at 37°C or on ice. Surface staining of MHC II and CD80 was performed after FITC-OVA incubation. Each dot represents an individual animal, and the bar represents the mean (n=4). **(C)** FO B cells or ABCs were pre-treated with metformin for 3 hours prior to incubation with OVA. After OVA incubation, naïve CD4+ T cells, which were isolated from OTII mice, were added to B cells and cultured for 4 days. The percentage of live T cells and Tfh cells (CXCR5+/PD1+/BCL6+/IL-21+) was identified by flow cytometry and plotted. Each dot represents an individual animal, and the bar represents the mean (n=3). One-way ANOVA was used with Sidak's correction for multiple comparisons. TC mice were treated with metformin or saline for one week and spleens were collected for ABCs isolation. **(D)** Percent of ABCs was plotted (n=4). **(E)** ABCs were isolated and OVA uptake was measured by flow cytometry. OVA+ ABCs was calculated based on the ice incubation control (n=4). **(F)** ABCs were isolated and OVA protein was incubated for 3 hours. Then, naïve CD4+ T cells from OT II mice and ABCs were co-culture for 4 days. Viability, CD44+ T cells and Tfh cells were measured as described in **(C)** (n=4). Each dot represents an individual animal, and the bar represents the mean. One-way ANOVA was used for statistics and Sidak's correction was applied for multiple comparisons.

suggests that ABCs can activate T cells more efficiently than naïve B cells. Marrack and colleagues showed that CD11c+ B cells express distinct chemokine receptors, reside at the T-B border and activate T cells in aged female mice as well as in *B6.Nba2* lupus mice (14). Li and colleagues found that CD11c+ B cells are required for the expansion of Tfh cells in B cell specific SHIP-deficient lupus mice (15). Our study confirmed ABCs act as efficient APCs leading to an activating antigen-specific T cell. OVA uptake maybe a common function of ABCs, since ABCs from aged non-lupus mice also performed this function. Interestingly, the antigen-specific T cell activation was much weaker in non-lupus mice. It may reflect a difference of OVA processing or cytokine production between lupus mice and non-lupus mice.

Our study confirmed several features of ABCs, including the increased expression of costimulatory molecules and antigen uptake needed for T cell activation and an increased frequency of class-switched ABCs in lupus-prone TC mice. Although there was an increase in class-switched populations (~10% of total ABCs), most ABCs express high levels of IgD and IgM. It is important to

understand whether those class-switched ABCs and IgD<sup>hi</sup>IgM+ ABCs have different functions and whether any of subset contributes to lupus development or progression. A recent study characterized CD11c+ ABCs in the MRL/lpr mouse model of lupus (40). In this study, heterogeneity of ABCs was found with respect to expression of integrins and memory or plasmablast markers. Many genes expressed in ABCs in this study were also increased in ABCs in our study. Our data also revealed additional pathways that are enriched in ABCs, including amino acid transporters and cytokine receptor signaling.

We also made some novel observations, such as an increased hypoxic pathway, increased mitochondrial metabolism and mitochondrial ROS production, along with preferential induction of Tfh cells. T cell activation and Tfh differentiation by ABCs may reflect in part an autoimmune background since this function was markedly diminished in ABCs from non-lupus background. Since OVA uptake occurs similarly in ABCs from both lupus and non-lupus mice, antigen processing may differ depending on the genetic background of strain. It needs to be determined whether OVA is

taken into an endo-lysosomal compartment in ABCs in lupus mice but not in non-lupus mice. Comparison of ABCs to GC B cells highlighted the uniqueness of ABCs as APCs. GC B cells express higher levels of MHC II and CD86, but CD80 expression is much lower in GC B cells than ABCs. The cytokine profile of ABCs and GC B cells are different; GC B cells do not produce IL-10 or IL-1 $\beta$ . Both GC B cells and ABCs express high levels of genes involved in glycolysis, suggesting both B cell types have enhanced glycolysis. An increased levels of Hif1a and Mthfd2 expression was observed only in ABCs, suggesting a metabolic difference between these two activated B cell populations.

ABCs have elevated expression of genes involved in phagocytosis, antigen presentation and plasma membrane invagination. CD36 and AXL are cell surface molecules on ABCs, involved in antigen uptake in innate immune cells and have been suggested to help clear apoptotic debris in DEF6/Swap70 double knockout mice (41). CD36 is a scavenger receptor and facilitates uptake of fatty acids (42). This is a key step in energy metabolism and may explain the increased lipid metabolites in ABCs (Supplementary Figure 4). In line with a role of CD36 in lipid metabolism, a recent study showed an expansion of T-bet+ B cells in adipose tissue where they contribute to the metabolic disorder in obese mice (43). Despite their high level of CD36 expression, CD36 was not responsible for uptake of OVA or dextran.

Another observation we made was the metabolic difference between ABCs and FO B cells. Human circulating ABCs are suggested to be atypical memory B cells, and memory B cells are relatively quiescent metabolically. AMPK appears to be important in mitochondrial homeostasis and maintaining memory B cells (44). Therefore, we hypothesized that CD11c+ ABCs might utilize mitochondria or lipid oxidation for their energy production. In contrast to this hypothesis, ABCs exhibit increased metabolism in both mitochondrial respiration and glycolysis compared to naive FO B cells even without ex vivo stimulation. This is consistent with a recent study of the bm2 mouse model of SLE. The investigators showed an increased glycolytic capacity of ABCs in this mouse; moreover, inhibition of heightened glycolysis by 2-DG administration inhibited ABC formation and decreased the autoantibody production (45), suggesting that the glycolytic pathway is required for ABC generation, ABC survival or antibody production by ABCs in lupus mice. This phenotype was observed in ABCs from another lupus mouse model, B6.lpr, but not in ABCs from aged female mice from a non-lupus background. We also compared metabolic status in ABCs and FO B cells from NZB/W F1 lupus mice; enhanced glucose uptake and mitochondrial activation were observed in ABCs compared to FO B cells (data not shown). Increased mitochondrial ROS production was observed in ABCs from both autoimmune and non-autoimmune mice. These data suggest that a disease-dependent metabolic adaptation in ABCs exists. It is unclear whether the metabolic difference in ABCs between lupus mice and aged non-lupus mice is due to a different cytokine milieu in diseased and in healthy aging or different precursors (naive B cells or memory B cells) or different genetic influences. Intermediate levels of ROS can serve as signaling molecules and are important for lymphocyte activation augmenting intracellular signaling pathways downstream of BCR

(46). Elevated ROS can modify intracellular molecules and oxidized mitochondrial DNA which can be translocated into cytoplasm, leading to an activation of the inflammasome and IL-1 $\beta$  secretion in macrophages (47). We observed an increased secretion of IL-1 $\beta$  by ABCs, which may be due to an elevation of ROS and increased inflammasome activity.

The observation that metformin treatment prevents antigen uptake and Tfh differentiation is novel, too. *In vitro* treatment with metformin (few hours) did not affect the expression of costimulatory molecules or cytokine production. *In vivo* exposure to metformin (1 week) did not change the frequency of B cell subsets, including FO B, MZ B, GC B and CD138<sup>++</sup> PCs in TC mice. We found, however, a trend toward fewer ABCs in metformin treated TC mice. Moreover, those ABCs exhibit reduced OVA uptake and T cell activation capacity. The mechanisms by which metformin alters ABC function need to be further studied. Metformin is a therapeutic option for several diseases. The Met LUPUS trial, an open-labelled clinical trial, showed that metformin reduces disease flares in SLE patients (48). Metformin treatment can suppress disease progression in *Roquin*<sup>san/san</sup> mice (37). In TC mice, metformin can prevent disease onset and reverse the disease progression when used with 2-DG, an irreversible inhibitor of glucose transporter (35). The combination of metformin and 2-DG actively suppresses CD4+ effector T cells or memory T cell differentiation/accumulation, but the direct effect of these drugs on B cells was not addressed. Indeed, the mechanism of metformin on B cells or B cell subsets is still an open question. Our study shows that metformin can directly affect the function of ABCs *in vitro* by reducing antigen uptake and CD80 expression, leading to reduced Tfh differentiation. Surprisingly, there was no change in cytokine production or in the level of expression of other costimulatory molecules or MHC II following metformin treatment. The mechanism by which metformin causes the decrease in antigen uptake and CD80 expression requires further study.

## Data availability statement

The datasets presented in this study can be found in online repositories. The names of the repository/repositories and accession number(s) can be found below: <https://www.ncbi.nlm.nih.gov/geo/>, GSE214185.

## Ethics statement

The animal study was approved by The Feinstein Institutes for Medical Research (FIMR) institutional animal care and use committee (IACUC). The study was conducted in accordance with the local legislation and institutional requirements.

## Author contributions

SK conceived and designed the overall study and interpreted the results. IR performed the experiments and analyzed the data. AS

and KL performed the RNA-sequencing analyses. VK designed and performed the metabolomic analyses. SK, IR, YA and BD participated in the interpretation of the study, writing and critical review of the manuscript. All authors contributed to the article and approved the submitted version.

## Funding

This study was supported by NIAMS, US National Institute for Health (R01 AR074565, U19 AI144306, and P01 AI148102 to SK and BD).

## Acknowledgments

We thank C. Colon for assistance with flow cytometry; JW Choi at the Oregon State University for consultation and analysis of metabolomics, and JH Kim at the FIMR for assistance of Metabolomic analysis.

## References

- Jenks SA, Cashman KS, Zumaquero E, Marigorta UM, Patel AV, Wang X, et al. Distinct effector B cells induced by unregulated toll-like receptor 7 contribute to pathogenic responses in systemic lupus erythematosus. *Immunity* (2018) 49:725–739 e6. doi: 10.1016/j.immuni.2018.08.015
- Rubtsov AV, Rubtsova K, Fischer A, Meehan RT, Gillis JZ, Kappler JW, et al. Toll-like receptor 7 (TLR7)-driven accumulation of a novel CD11c(+) B-cell population is important for the development of autoimmunity. *Blood* (2011) 118:1305–15. doi: 10.1182/blood-2011-01-331462
- Rubtsova K, Rubtsov AV, Thurman JM, Mennona JM, Kappler JW, Marrack P. B cells expressing the transcription factor T-bet drive lupus-like autoimmunity. *J Clin Invest* (2017) 127:1392–404. doi: 10.1172/JCI91250
- Dai X, James RG, Habib T, Singh S, Jackson S, Khim S, et al. A disease-associated PTPN22 variant promotes systemic autoimmunity in murine models. *J Clin Invest* (2013) 123:2024–36. doi: 10.1172/JCI66963
- Mouat IC, Morse ZJ, Shanina I, Brown KL, Horwitz MS. Latent gammaherpesvirus exacerbates arthritis through modification of age-associated B cells. *Elife* (2021) 10. doi: 10.7554/eLife.67024
- Rubtsova K, Rubtsov AV, van Dyk LF, Kappler JW, Marrack P. T-box transcription factor T-bet, a key player in a unique type of B-cell activation essential for effective viral clearance. *Proc Natl Acad Sci U.S.A.* (2013) 110:E3216–24. doi: 10.1073/pnas.1312348110
- Mouat IC, Goldberg E, Horwitz MS. Age-associated B cells in autoimmune diseases. *Cell Mol Life Sci* (2022) 79:402. doi: 10.1007/s00018-022-04433-9
- Rakhmanov M, Keller B, Gutenberger S, Foerster C, Hoenig M, Driessen G, et al. Circulating CD21low B cells in common variable immunodeficiency resemble tissue homing, innate-like B cells. *Proc Natl Acad Sci USA* (2009) 106:13451–6. doi: 10.1073/pnas.0901984106
- Tipton CM, Fucile CF, Darce J, Chida A, Ichikawa T, Gregoret I, et al. Diversity, cellular origin and autoreactivity of antibody-secreting cell population expansions in acute systemic lupus erythematosus. *Nat Immunol* (2015) 16:755–65. doi: 10.1038/ni.3175
- Wang S, Wang J, Kumar V, Karnell JL, Naiman B, Gross PS, et al. IL-21 drives expansion and plasma cell differentiation of autoreactive CD11c(hi)T-bet(+) B cells in SLE. *Nat Commun* (2018) 9:1758. doi: 10.1038/s41467-018-03750-7
- Hao Y, O'Neill P, Naradikian MS, Scholz JL, Cancro MP. A B-cell subset uniquely responsive to innate stimuli accumulates in aged mice. *Blood* (2011) 118:1294–304. doi: 10.1182/blood-2011-01-330530
- Song W, Antao OQ, Condif E, Sanchez GM, Chernova I, Zembrzuski K, et al. Development of Tbet- and CD11c-expressing B cells in a viral infection requires T follicular helper cells outside of germinal centers. *Immunity* (2022) 55:290–307 e5. doi: 10.1016/j.immuni.2022.01.002

## Conflict of interest

The authors declare that the research was conducted in the absence of any commercial or financial relationships that could be construed as a potential conflict of interest.

## Publisher's note

All claims expressed in this article are solely those of the authors and do not necessarily represent those of their affiliated organizations, or those of the publisher, the editors and the reviewers. Any product that may be evaluated in this article, or claim that may be made by its manufacturer, is not guaranteed or endorsed by the publisher.

## Supplementary material

The Supplementary Material for this article can be found online at: <https://www.frontiersin.org/articles/10.3389/fimmu.2023.1241531/full#supplementary-material>

- Murakami Y, Fukui R, Tanaka R, Motoi Y, Kanno A, Sato R, et al. Anti-TLR7 antibody protects against lupus nephritis in NZBWF1 mice by targeting B cells and patrolling monocytes. *Front Immunol* (2021) 12:777197. doi: 10.3389/fimmu.2021.777197
- Rubtsov AV, Rubtsova K, Kappler JW, Jacobelli J, Friedman RS, Marrack P. CD11c-expressing B cells are located at the T cell/B cell border in spleen and are potent APCs. *J Immunol* (2015) 195:71–9. doi: 10.4049/jimmunol.1500055
- Zhang W, Zhang H, Liu S, Xia F, Kang Z, Zhang Y, et al. Excessive CD11c(+) Tbet(+) B cells promote aberrant TFH differentiation and affinity-based germinal center selection in lupus. *Proc Natl Acad Sci U.S.A.* (2019) 116:18550–60. doi: 10.1073/pnas.1901340116
- Watanabe-Fukunaga R, Brannan CI, Copeland NG, Jenkins NA, Nagata S. Lymphoproliferation disorder in mice explained by defects in Fas antigen that mediates apoptosis. *Nature* (1992) 356:314–7. doi: 10.1038/356314a0
- Moran AE, Holzapfel KL, Xing Y, Cunningham NR, Maltzman JS, Punt J, et al. T cell receptor signal strength in Treg and iNKT cell development demonstrated by a novel fluorescent reporter mouse. *J Exp Med* (2011) 208:1279–89. doi: 10.1084/jem.20110308
- Kim V, Lee K, Tian H, Jang SH, Diamond B, Kim SJ. IL-17-producing follicular Th cells enhance plasma cell differentiation in lupus-prone mice. *JCI Insight* (2022) 7. doi: 10.1172/jci.insight.157332
- Drummen GP, van Liebergen LC, Op den Kamp JA, Post JA. C11-BODIPY(581/591), an oxidation-sensitive fluorescent lipid peroxidation probe: (micro)spectroscopic characterization and validation of methodology. *Free Radic Biol Med* (2002) 33:473–90. doi: 10.1016/S0891-5849(02)00848-1
- Dobin A, Davis CA, Schlesinger F, Drenkow J, Zaleski C, Jha S, et al. STAR: ultrafast universal RNA-seq aligner. *Bioinformatics* (2013) 29:15–21. doi: 10.1093/bioinformatics/bts635
- Love MI, Huber W, Anders S. Moderated estimation of fold change and dispersion for RNA-seq data with DESeq2. *Genome Biol* (2014) 15:550. doi: 10.1186/s13059-014-0550-8
- Subramanian A, Tamayo P, Mootha VK, Mukherjee S, Ebert BL, Gillette MA, et al. Gene set enrichment analysis: a knowledge-based approach for interpreting genome-wide expression profiles. *Proc Natl Acad Sci U.S.A.* (2005) 102:15545–50. doi: 10.1073/pnas.0506580102
- Liberzon A, Birger C, Thorvaldsdottir H, Ghandi M, Mesirov JP, Tamayo P. The Molecular Signatures Database (MSigDB) hallmark gene set collection. *Cell Syst* (2015) 1:417–25. doi: 10.1016/j.cels.2015.12.004
- Choi J, Shoaib M, Yin T, Nayyar G, Shinozaki K, Stevens JF, et al. Tissue-specific metabolic profiles after prolonged cardiac arrest reveal brain metabolome dysfunction predominantly after resuscitation. *J Am Heart Assoc* (2019) 8:e012809. doi: 10.1161/JAHA.119.012809

25. Yang R, Avery DT, Jackson KJL, Ogishi M, Benhsaien I, Du L, et al. Human T-bet governs the generation of a distinct subset of CD11c(high)CD21(low) B cells. *Sci Immunol* (2022) 7:eabq3277. doi: 10.1126/sciimmunol.abq3277
26. Ratliff M, Alter S, Frasca D, Blomberg BB, Riley RL. In senescence, age-associated B cells secrete TNFalpha and inhibit survival of B-cell precursors. *Aging Cell* (2013) 12:303–11. doi: 10.1111/accel.12055
27. Smith MJ, Packard TA, O'Neill SK, Hinman RM, Rihaneck M, Gottlieb PA, et al. Detection and enrichment of rare antigen-specific B cells for analysis of phenotype and function. *J Vis Exp* (2017). doi: 10.3791/55382
28. Junker F, Gordon J, Qureshi O. Fc gamma receptors and their role in antigen uptake, presentation, and T cell activation. *Front Immunol* (2020) 11:1393. doi: 10.3389/fimmu.2020.01393
29. Lim JJ, Grinstein S, Roth Z. Diversity and versatility of phagocytosis: roles in innate immunity, tissue remodeling, and homeostasis. *Front Cell Infect Microbiol* (2017) 7:191. doi: 10.3389/fcimb.2017.00191
30. Huntington JA, Stein PE. Structure and properties of ovalbumin. *J Chromatogr B Biomed Sci Appl* (2001) 756:189–98. doi: 10.1016/S0378-4347(01)00108-6
31. Ashouri JF, Weiss A. Endogenous nur77 is a specific indicator of antigen receptor signaling in human T and B cells. *J Immunol* (2017) 198:657–68. doi: 10.4049/jimmunol.1601301
32. Chtanova T, Tangye SG, Newton R, Frank N, Hodge MR, Rolph MS, et al. T follicular helper cells express a distinctive transcriptional profile, reflecting their role as non-Th1/Th2 effector cells that provide help for B cells. *J Immunol* (2004) 173:68–78. doi: 10.4049/jimmunol.173.1.68
33. Zou C, Wang Y, Shen Z. 2-NBDG as a fluorescent indicator for direct glucose uptake measurement. *J Biochem Biophys Methods* (2005) 64:207–15. doi: 10.1016/j.jbbm.2005.08.001
34. Choi SC, Morel L. Immune metabolism regulation of the germinal center response. *Exp Mol Med* (2020) 52:348–55. doi: 10.1038/s12276-020-0392-2
35. Yin Y, Choi SC, Xu Z, Perry DJ, Seay H, Croker BP, et al. Normalization of CD4+ T cell metabolism reverses lupus. *Sci Transl Med* (2015) 7:274ra18. doi: 10.1126/scitranslmed.aaa0835
36. Bridges HR, Jones AJ, Pollak MN, Hirst J. Effects of metformin and other biguanides on oxidative phosphorylation in mitochondria. *Biochem J* (2014) 462:475–87. doi: 10.1042/BJ20140620
37. Lee SY, Moon SJ, Kim EK, Seo HB, Yang EJ, Son HJ, et al. Metformin Suppresses Systemic Autoimmunity in Roquin(san/san) Mice through Inhibiting B Cell Differentiation into Plasma Cells via Regulation of AMPK/mTOR/STAT3. *J Immunol* (2017) 198:2661–70. doi: 10.4049/jimmunol.1403088
38. Hawley SA, Ross FA, Chevztzoff C, Green KA, Evans A, Fogarty S, et al. Use of cells expressing gamma subunit variants to identify diverse mechanisms of AMPK activation. *Cell Metab* (2010) 11:554–65. doi: 10.1016/j.cmet.2010.04.001
39. Mustelin T, Lood C, Giltiay NV. Sources of pathogenic nucleic acids in systemic lupus erythematosus. *Front Immunol* (2019) 10:1028. doi: 10.3389/fimmu.2019.01028
40. Nickerson KM, Smita S, Hoehn KB, Marinov AD, Thomas KB, Kos JT, et al. Age-associated B cells are heterogeneous and dynamic drivers of autoimmunity in mice. *J Exp Med* (2023) 220. doi: 10.1084/jem.20221346
41. Ricker E, Manni M, Flores-Castro D, Jenkins D, Gupta S, Rivera-Correa J, et al. Altered function and differentiation of age-associated B cells contribute to the female bias in lupus mice. *Nat Commun* (2021) 12:4813. doi: 10.1038/s41467-021-25102-8
42. Xu S, Jay A, Brunaldi K, Huang N, Hamilton JA. CD36 enhances fatty acid uptake by increasing the rate of intracellular esterification but not transport across the plasma membrane. *Biochemistry* (2013) 52:7254–61. doi: 10.1021/bi400914c
43. Hagglof T, Vanz C, Kumagai A, Dudley E, Ortega V, Siller M, et al. T-bet(+) B cells accumulate in adipose tissue and exacerbate metabolic disorder during obesity. *Cell Metab* (2022) 34:1121–1136 e6. doi: 10.1016/j.cmet.2022.07.002
44. Brookens SK, Cho SH, Basso PJ, Boothby MR. AMPKalpha1 in B cells dampens primary antibody responses yet promotes mitochondrial homeostasis and persistence of B cell memory. *J Immunol* (2020) 205:3011–22. doi: 10.4049/jimmunol.1901474
45. Han X, Gu S, Hong SM, Jiang Y, Zhang J, Yao C, et al. Amelioration of autoimmunity in a lupus mouse model by modulation of T-bet-promoted energy metabolism in pathogenic age/autoimmune-associated B cells. *Arthritis Rheumatol* (2023) 75:1203–15. doi: 10.1002/art.42433
46. Feng YY, Tang M, Suzuki M, Gunasekara C, Anbe Y, Hiraoka Y, et al. Essential role of NADPH oxidase-dependent production of reactive oxygen species in maintenance of sustained B cell receptor signaling and B cell proliferation. *J Immunol* (2019) 202:2546–57. doi: 10.4049/jimmunol.1800443
47. Egawa T, Bhattacharya D. Regulation of metabolic supply and demand during B cell activation and subsequent differentiation. *Curr Opin Immunol* (2019) 57:8–14. doi: 10.1016/j.coi.2018.10.003
48. Sun F, Geng S, Wang H, Wang H, Liu Z, Wang X, et al. Effects of metformin on disease flares in patients with systemic lupus erythematosus: *post hoc* analyses from two randomised trials. *Lupus Sci Med* (2020) 7. doi: 10.1136/lupus-2020-000429